

## Supporting Information

for

### **Biaxial Pseudorotaxane Secondary Assembly for Phosphorescent Cellular Imaging**

Yao-Hua Liu, Mian Tang, Xiaolu Zhou and Yu Liu\*

*College of Chemistry, State Key Laboratory of Elemento-Organic Chemistry, Nankai*

*University, Tianjin 300071, P. R. China*

*\*E-mail: [yuliu@nankai.edu.cn](mailto:yuliu@nankai.edu.cn)*

## Instruments.

NMR spectra were recorded on Bruker 400 MHz instrument, and chemical shifts were recorded in parts per million (ppm). High resolution mass (HRMS) spectra were performed on Varian 7.0T FTMS with ESI or MALDI source. TEM images were acquired by a high-resolution transmission electron microscope (Philips Tecnai G2 20S-TWIN microscope) operating at an accelerating voltage of 200 keV. The samples were prepared by placing a drop of solution onto a carbon-coated copper grid and air-dried. The morphological information was directly obtained from the fresh TEM samples without staining. Transmission spectra were recorded on a Shimadzu UV-3600 spectrophotometer in a quartz cell (light path 10 mm) at 25 °C with a PTC-348WI temperature controller. Dynamic light scattering (DLS) was recorded on BI-200SM (Brookhaven Company) at 25 °C. Confocal fluorescence imaging was recorded with Olympus FV1000.

## Synthesis of BPTN

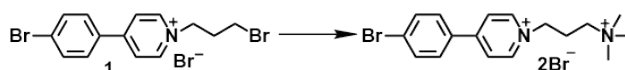


Figure S1 Synthetic route of BPTN.

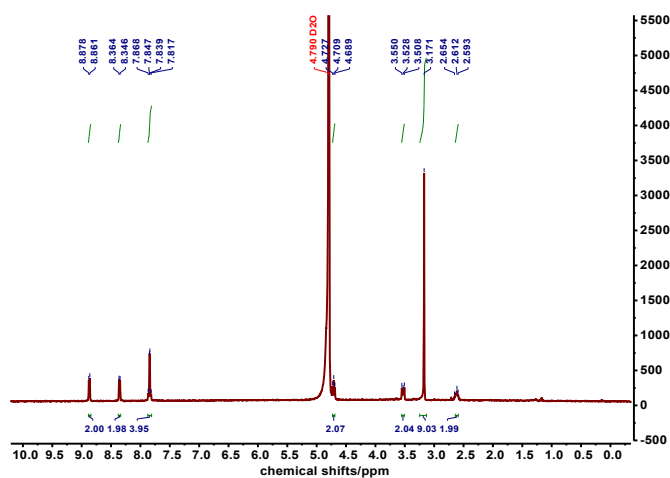


Figure S2 <sup>1</sup>H NMR spectra (400 MHz, D<sub>2</sub>O, 298K) of BPTN.

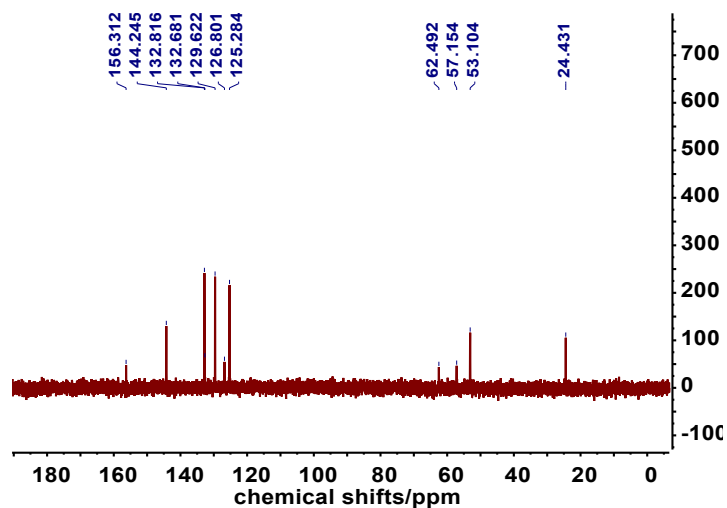


Figure S3  $^{13}\text{C}$  NMR spectra (100 MHz,  $\text{D}_2\text{O}$ , 298K) of BPTN.

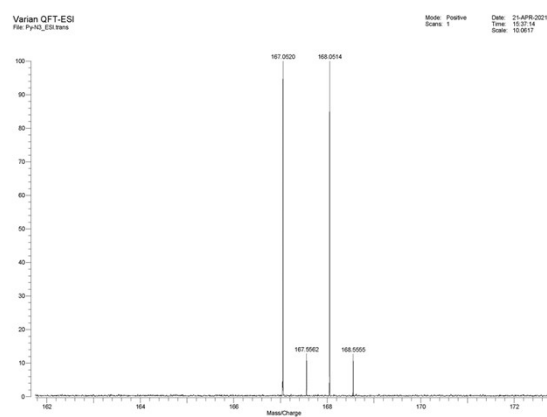


Figure S4 ESI-HRMS spectrum of BPTN.

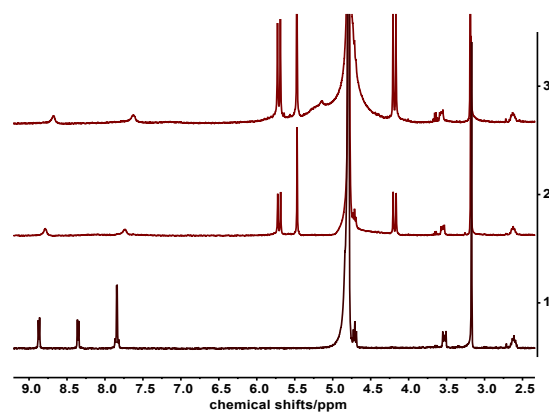


Figure S5  $^1\text{H}$  NMR spectroscopy of BPTN with (bottom) 0, (middle) 0.5 and (upper) 1 eq.  $\text{CB}[7]$  in  $\text{D}_2\text{O}$  at 298 K.

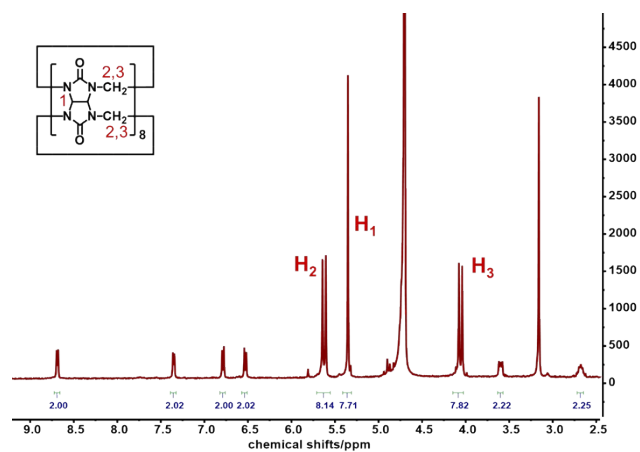


Figure S6  $^1\text{H}$  NMR spectra (400 MHz,  $\text{D}_2\text{O}$ , 298K) of  $\text{BPTN}@CB[8]$ . The binding ratio of BPTN and  $CB[8]$  can be calculated as 2:1 via the integral area.

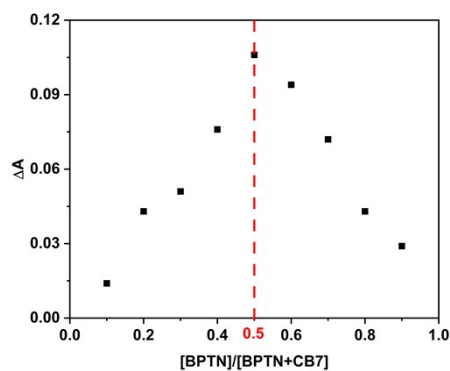


Figure S7 Job's plot of BPTN and  $CB[7]$  in PBS solution ( $[\text{BPTN}] + [\text{CB}[7]] = 50 \mu\text{M}$ ) at 298 K.

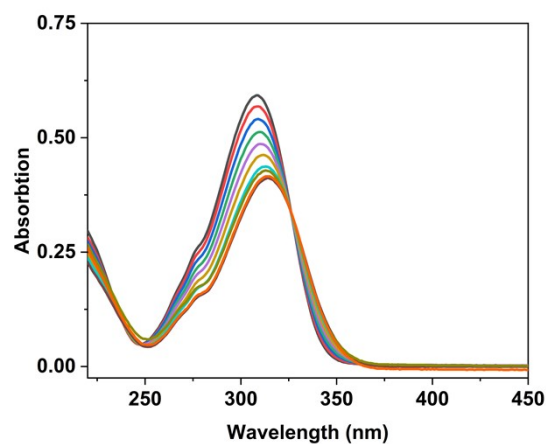


Figure S8 UV-vis absorption spectra of BPTN ( $[\text{BPTN}] = 20 \mu\text{M}$ ) upon the addition of  $CB[7]$  in PBS solution.

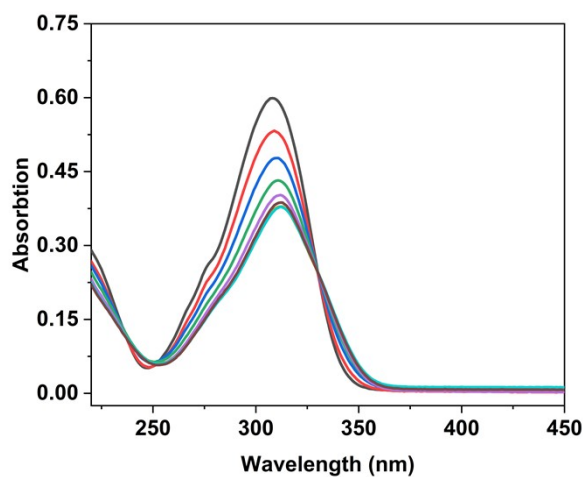


Figure S9 UV-vis absorption spectra of BPTN ( $[BPTN] = 20 \mu M$ ) upon the addition of CB[8] in PBS solution.

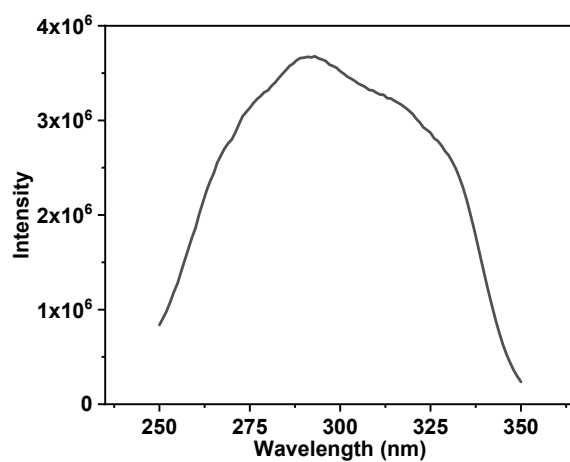


Figure S10 Excitation spectrum of BPPY-CB[8] in PBS solution ( $[BPTN] = 2[CB[8]] = 10 \mu M$ ).

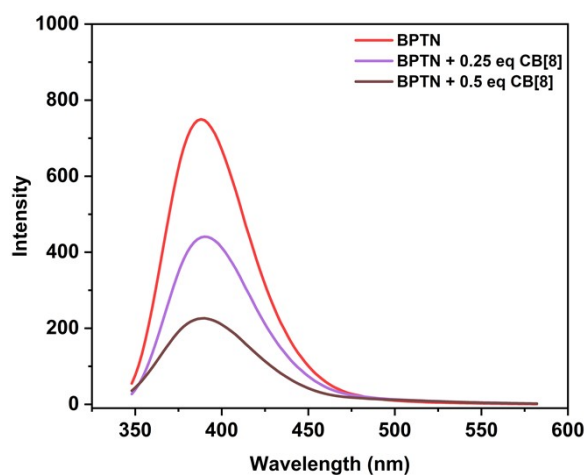


Figure S11 Fluorescence spectra of BPTN ( $10 \mu M$ ) and CB[8] at concentrations of 0, 2.5 and  $5 \mu M$ .

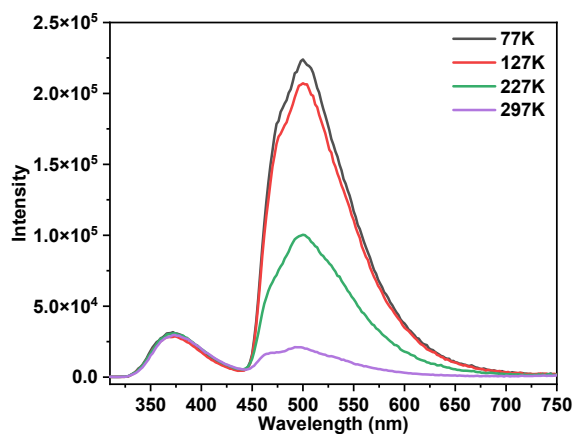


Figure S12 Photoluminescence spectra of BPTN@CB[8] at different temperature.

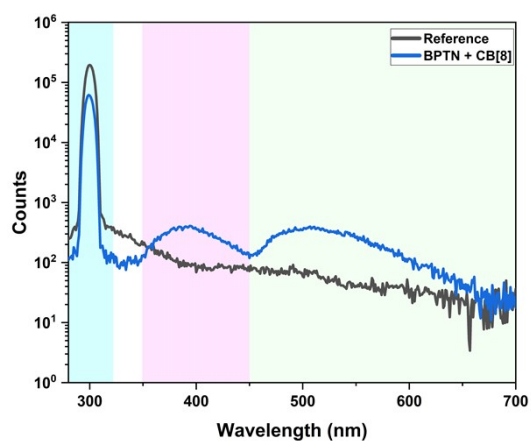


Figure S13 The quantum yield of BPTN@CB[8] ( $[BPTN] = 2[CB[8]] = 10 \mu M$ ).

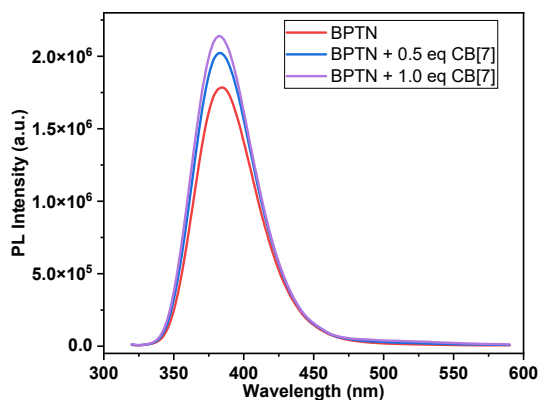


Figure S14 Photoluminescence spectra of BPTN (10 μM) and CB[7] at concentrations of 0, 5 and 10 μM.

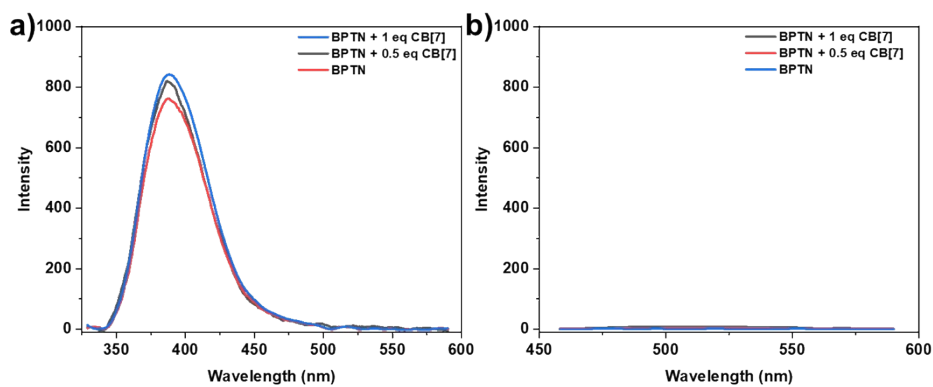


Figure S15 (a) Fluorescence spectra and (b) time-lapse photoluminescence spectra of BPTN (10  $\mu\text{M}$ ) and CB[7] at concentrations of 0, 5 and 10  $\mu\text{M}$ .

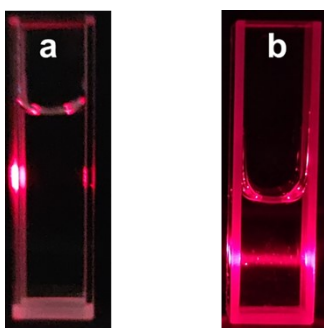


Figure S16 The Tyndall effect of solution of BPTN-CB[8] and BPTN-CB[8]@SSP[4] ( $[\text{BPTN}] = 2[\text{CB}[8]] = 10 \mu\text{M}$ ,  $[\text{SSP}[4]] = 20 \mu\text{M}$ ).

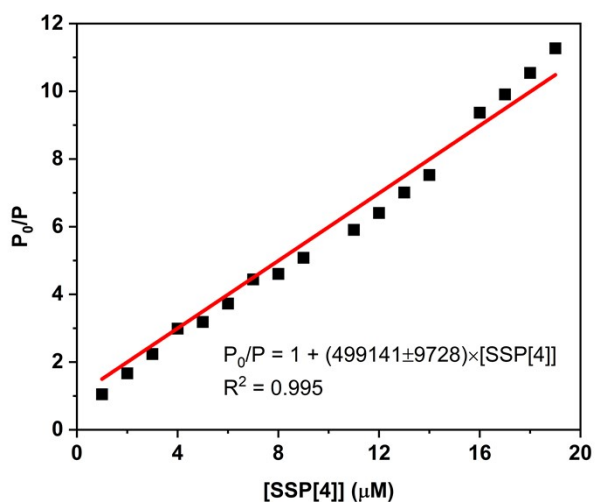


Figure S17 Stern-Volmer curves of BPTN-CB[8]@SSP[4] system.

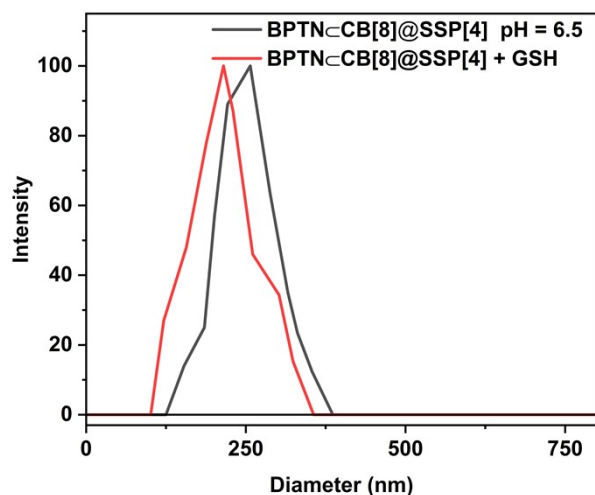


Figure S18 DLS data of BPTN-CB[8]@SSP[4] with GSH and BPTN-CB[8]@SSP[4] in pH = 6.5 solution ([BPTN] = 2[CB[8]] = 10  $\mu$ M, [SSP[4]] = 20  $\mu$ M, GSH = 2 mM).

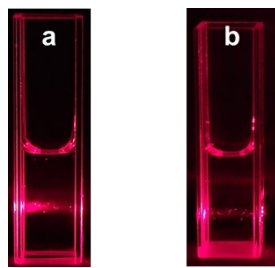


Figure S19 The Tyndall effect of solution of BPTN-CB[8]@SSP[4] with (a) GSH or (b) under pH = 6.5 ([BPTN] = 2[CB[8]] = 10  $\mu$ M, [SSP[4]] = 20  $\mu$ M).

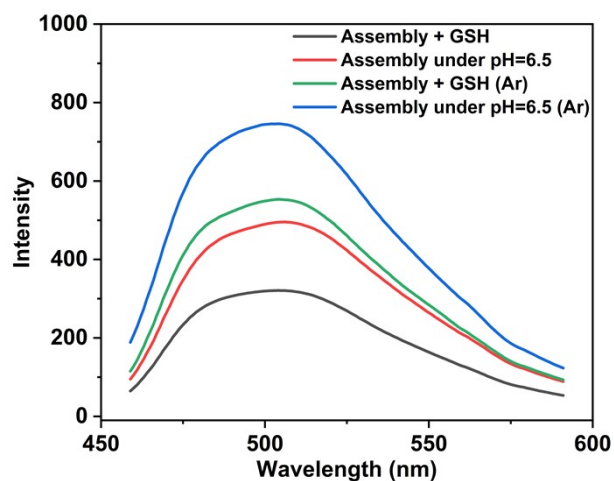


Figure S20 Time-lapse photoluminescence spectra of BPTN-CB[8]@SSP[4] with GSH or under pH = 6.5 under argon atmosphere.



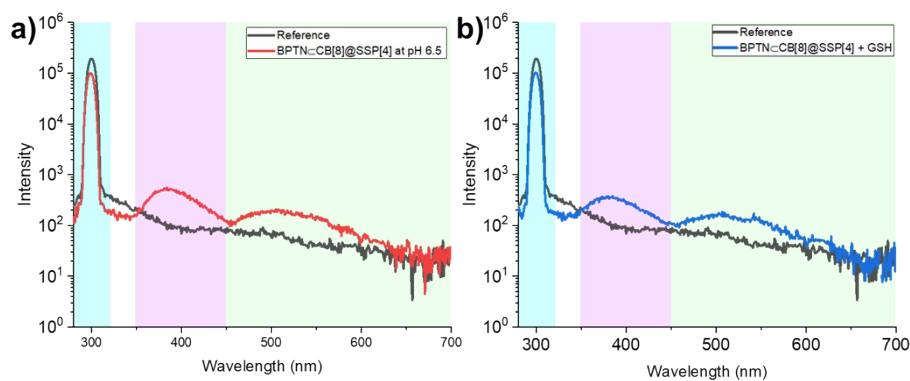


Figure S21 The quantum yield of BPTN-CB[8]@SSP[4] with (a) GSH or (b) adjusting pH to 6.5 ( $[BPTN] = 2[CB[8]] = 10 \mu M$ ,  $[SSP[4]] = 20 \mu M$ ,  $[GSH] = 2 \text{ mM}$ ).

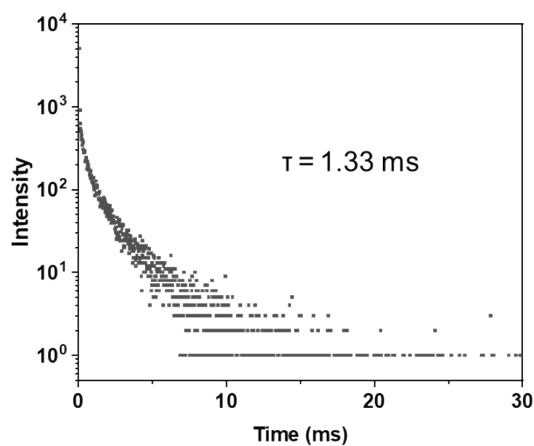


Figure S22 Time resolved photoluminescence decay curves of BPTN-CB[8]@SSP[4] at pH 6.5 in PBS solution ( $[BPTN] = 2[CB[8]] = 10 \mu M$ ,  $[SSP[4]] = 20 \mu M$ ).

Table S1 Phosphorescent properties of BPTN-CB[8] and BPTN-CB[8]@SSP[4] with GSH or adjusting pH to 6.5.

	Lifetime (ms)	Quantum Yield (%)	Normalized Intensity of Emission at 505 nm
BPTN-CB[8]	0.60	2.10	1.00
BPTN-CB[8]@SSP[4] with GSH	4.03	1.35	0.28
BPTN-CB[8]@SSP[4] at pH 6.5	1.33	0.81	0.46

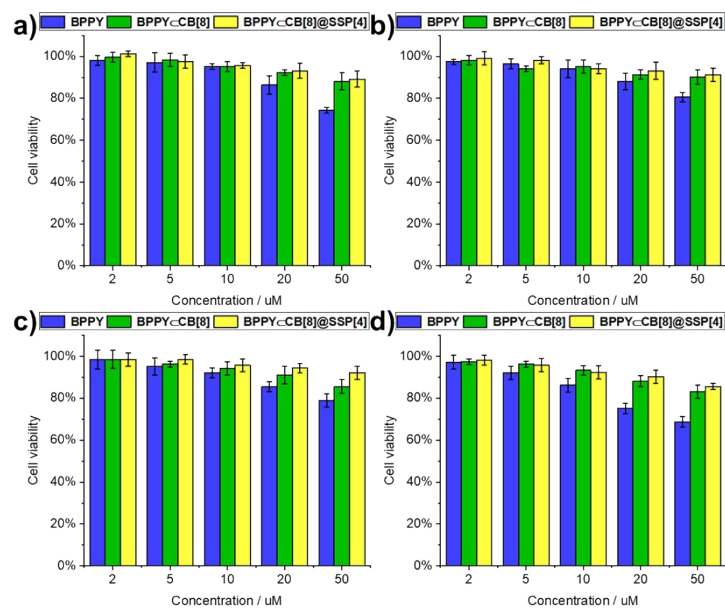


Figure S23 Cell viability of (a) A549, (b) HeLa, (c) MCF-7 and (d) 293T cells incubated with BPTN, BPTN-CB[8] and BPTN-CB[8]@SSP[4] at different concentration.

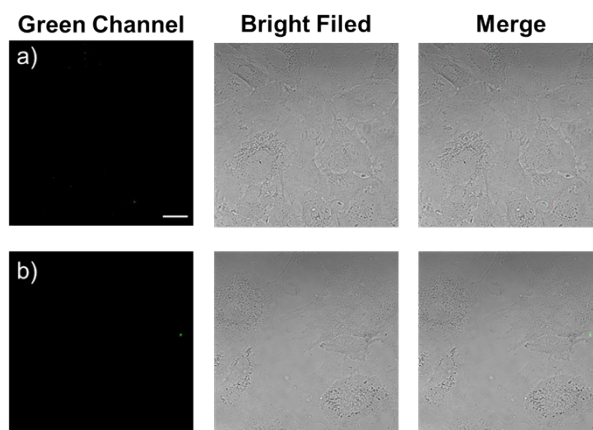


Figure S24 Confocal fluorescence images of living A549 cells incubated with (a) BPTN and (b) BPTN@SSP[4] (scale bar = 20  $\mu\text{m}$ ).